

A

		▼	
DPP3_HUMAN	300	WIQDKGPIVESYIGFIESYRDPFGSRGEFEG	330
DPP3_BOVIN	300	WIQDKGPIVESYIGFIESYRDPFGSRGEFEG	330
DPP3_RAT	300	WIQDKGPIVESYIGFIESYRDPFGSRGEFEG	330
DPP3_DROME	358	WIKDKGPVIETYIGFIETYRDPAGGRAEFEG	388
DPP3_DICDI	284	WIKDISPAVETNIGFIESYRDPYGVRGWEWEG	314
DPP3_YEAST	309	WVKDISPVIETNIGFIETYREPSGIIGEFES	339
DPP3_BACTN	291	WVKDLDSRIDFVNGFTESYGDPLGVKASWES	321
		:: . :: ** **:* * * ..:*	

B

		▼	
DPP3_HUMAN	498	KFSTIASSYEECRAESVGLYLCLHPQVLEIF	528
DPP3_BOVIN	498	KFSTIASSYEECRAESVGLYLCLHPRVLEIF	528
DPP3_RAT	498	KFSTIASSYEECRAESVGLYLCLNPQVLQIF	528
DPP3_DROME	554	KFGAIGSSYEECRAEAVGLYLSLQRDILEIF	584
DPP3_DICDI	482	VFKSLGSPMEECRAECCGIYLSPDEKILELF	512
DPP3_YEAST	507	KFGQLAGPFEECRAEVIAMFLLTNKKILDIF	537
DPP3_BACTN	466	ALKAYGSTIEEARADLFGLYYVADPKLVELK	496
		: .. **.**: .:: . ::::	

Figure S1 A multiple sequence alignment of the conserved regions containing the residues G313 (A) and R510 (B) from different DPPs III. Alignment was made using Clustal Omega (Sievers et al.) and UniProt sequences of DPPs III from: *Homo sapiens* (DPP3_HUMAN, accession code Q9NY33), *Bos taurus* (DPP3_BOVIN, F2Z4F5), *Rattus norvegicus* (DPP3_RAT, O55096), *Drosophila melanogaster* (DPP3_DROME, Q9VHR8), *Dictyostelium discoideum* (DPP3_DICDI, Q557H1), *Saccharomyces cerevisiae* (DPP3_YEAST, Q08225), and *Bacteroides thetaiotaomicron* (DPP3_BACTN, Q8A6N1). [Sievers, F., Wilm, A., Dineen, D.G., Gibson, T.J., Karplus, K., Li, W. Lopez, R., McWilliam, H., Remmert, M., Söding, J., et al. (2011). Fast, scalable generation of high-quality protein multiple sequence alignments using Clustal Omega. *Mol. Syst Biol.* 7, 539. doi:10.1038/msb.2011.75.]

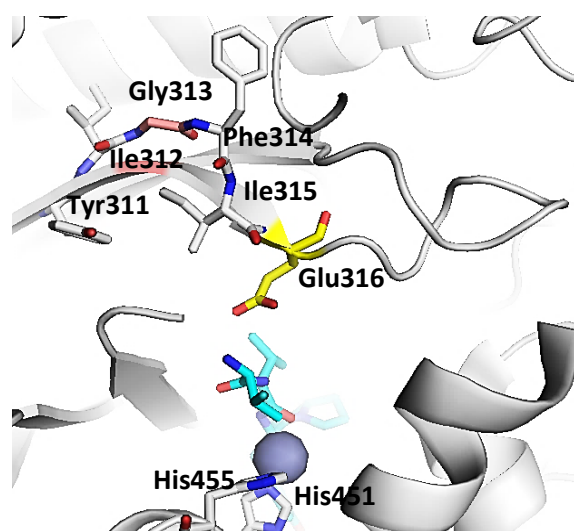


Figure S2 Position of highly conserved residue G313 (pink) in the bended β_6 sheet in the structure of h.DPP-III complex with opioid peptide tynorphin (cyan) (PDB code: 3T6B). Glu316 is represented in yellow and Zn^{2+} is represented as sphere.

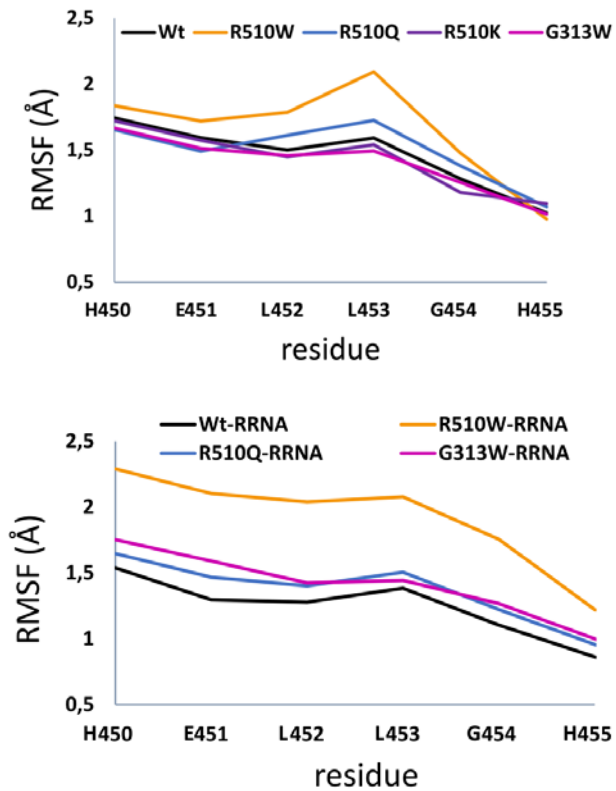


Figure S3 RMSF of the conserved HELGH motif calculated for 100 ns long MD simulations of the a) ligand free h.DPPIII variants in an open protein form and b) their complexes with the substrate Arg₂-2NA wherein the protein structure is closed.

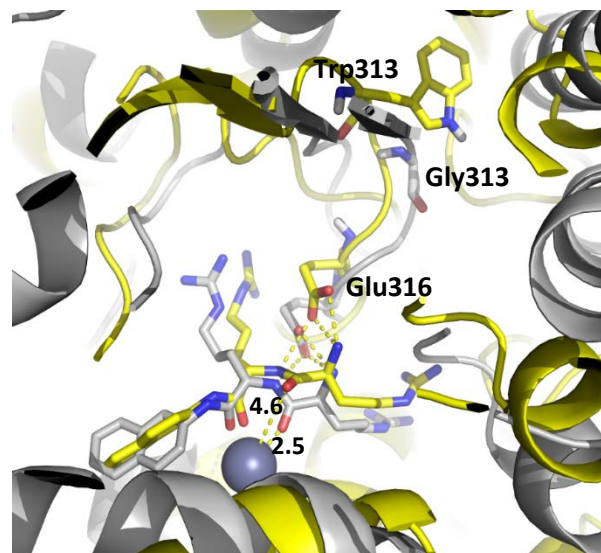


Figure S4 Overlay of the 100 ns simulated structures of the the complexes: WT h.DPP III - Arg₂-2NA (gray) and the G313W - Arg₂-2NA mutant (yellow) structures. The substrate and highly conserved Glu316 are given in stick representation and coloured respectively, and Zn²⁺ ions of both structures are overlaid (grey sphere). The close contacts of Glu316 with the substrate are shown by yellow dashed lines, and the distances of carbonyl group of the substrate from Zn²⁺ are shown.

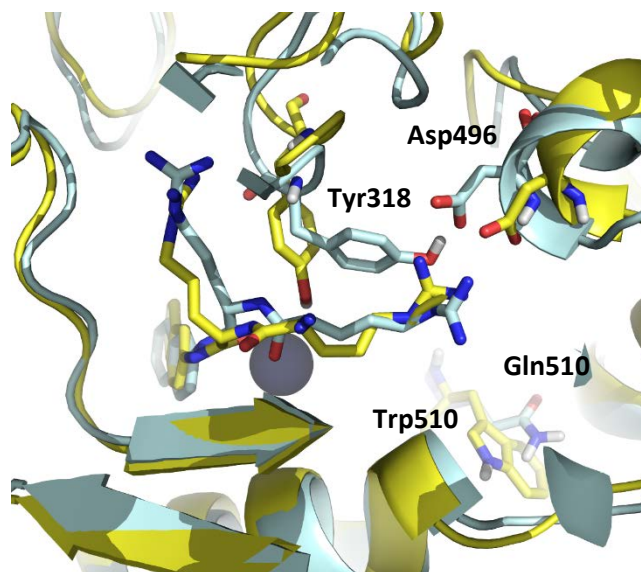


Figure S5 Overlay of the representative structures (obtained from clustering based on ligand RMSD) of the complexes: R510Q- Arg₂-2NA (light blue) and R510W Arg₂-2NA (yellow). The substrate and amino acid residues Tyr318 and Asp496 are displayed, as well as the position of mutated residues at the position 510.

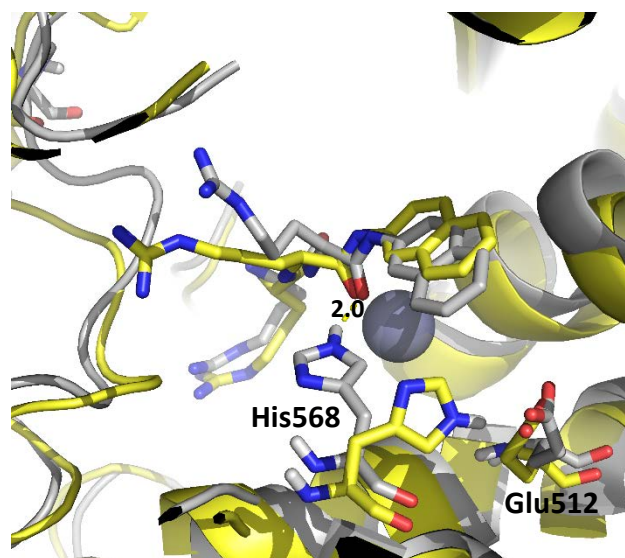


Figure S6 Orientation of His568 in the representative structures (obtained from clustering based on substrate RMSD) of the h.DPP III- Arg₂-2NA (WT - Arg₂-2NA) (gray) and G313W - Arg₂-2NA (yellow) complexes.

Table S1 Simulated h.DPP III variants and their complexes with Arg₂-2NA. The Zn²⁺ coordination and the range of radius of gyration determined during entire MD simulation is given in the last five columns, respectively. Letters 'm' and 'b' denote how carboxylate groups of glutamates 451 and 508 coordinate the metal cation: monodentately (via one of the carboxylate O atoms) or bidentately (via both carboxylate O atoms), respectively. For each ligand free variant as well as its complex with Arg₂-2NA there are two replica. All simulations were performed using the ff14SB force field and following the same procedure.

System	(t/ns)		Zn ²⁺ Coordination				R _{gyr}
	CMD	AMD	H450	H455	E451	E508	Range (Å)
WT-1	50	50	+	+	m	m	26.9-28.2
WT-2	50	50	+	+	m	m	26.9-28.4
G313W-1	50	50	+	+	m	m/b	26.7-28.5
G313W-2	50	50	+	+	m	b/m	26.7-28.5
G313A-1	50	50	+	+	m	m	26.4-28.5
G313A-2	50	50	+	+	m	m	26.5-28.5
R510W-1	50	50	+	+	m	m	26.4-28.3
R510W-2	50	50	+	+	m	m	26.2-28.3
R510Q-1	50	50	+	+ -	m	m	27.2-28.4
R510Q-2	50	50	+	+	m	m	27.0-28.4
R510K-1	50	50	+	+ -	m	m	26.3-28.0
R510K-2	50	50	+	+	m	b	26.3-28.0
WT-RRNA-1	50	50	+	+	m	b	24.9-25.5
WT-RRNA-2	50	50	+	+	m	b	24.9-25.6
G313W-RRNA-1	50	50	+	+	b	b	24.8-25.6
G313W-RRNA-2	50	50	+	+	m	b	25.0-25.5
R510W-RRNA-1	50	50	+	+	m	b	24.9-25.6
R510W-RRNA-2	50	50	+	+	m	b	25.0-25.7
R510Q-RRNA-1	50	50	+	+	b	b	24.8-25.5
R510Q-RRNA-2	50	50	+	+	m	b/m	24.8-25.5
R510K-RRNA-1	50	50	+	+	m	b/m	24.9-25.7
R510K-RRNA-2	50	50	+	+	m	b	24.8-25.6
G313A-RRNA-1	50	50	+	+	b	b	24.9-25.5
G313A-RRNA-2	50	50	+	+	b	b	24.9-25.5